DESIGN CHARACTERISTICS OF THE K=800 SUPERCONDUCTING CYCLOTRON AT M.S.U.*

F. Resmini, G. Bellomo, E. Fabrici, H.G. Blosser, and D. Johnson
Cyclotron Laboratory, Michigan State University
East Lansing, Michigan 48824

Introduction

Design work on the proposed K=800, K_F=400, superconducting cyclotron at MSU has progressed to the point where overall machine characteristics are firmly established. The main purpose[1] of the machine is to serve as a booster for the K=500 cyclotron, now under construction. In this respect, let us recall that the design goal is to achieve maximum beam energies of 200 MeV/n for fully stripped light ions, and typically 30-40 MeV/n for heavy ions like uranium. Energy variability down to about 50 MeV/n and 4-5 MeV/n, again for light and heavy ions respectively, is also required to ensure some overlap with beam energies delivered by the K = 500 in stand-alone mode.

Such an extreme range of beam energies, from very relativistic to non relativistic ones, demands a careful analysis of the intrinsic physics of the machine. Coupling to the first cyclotron, with the associated problems of beam injection and definition of the operating modes of both cyclotrons, is also a complex topic, and has indeed a number of consequences on the machine characteristics.

At this stage we believe that all major topics have been explored in sufficient detail so as to produce a consistent design. In the process, some unexpected findings led us to introduce a few unusual features, and it is the purpose of this paper to discuss the rationale behind them. For the sake of clarity, however, we shall first review the overall design as it stands now, turning thereafter to a detailed analysis of the single issues.

Outline of the Machine Design

A summary of the main cyclotron parameters is given in Table I, while a schematic horizontal layout and a vertical section are presented in Figs. 1 and 2. Choice of the pole radius, minimum hill gap, and sector spiral constant was mainly determined by the axial focussing requirements for 200 MeV/n fully stripped ions. A careful analysis of a number of different configurations indicated that the 41" pole radius was the minimum possible, and it has indeed been associated with a tight spiral and a hill gap of 2.5". In fact, a gap of 3" would already require, for the same spiral, a pole radius of 44"-45" at least. Average field $\bar{B}(r)$, ν_z and phase are presented as a function of radius in Fig. 3 for two examples of 200 MeV/n and 20 MeV/n beams, showing that the present configuration meets all acceleration requirements.

Table I. Main K=800 parameters.

Pole radius	41"
Outer hill radius	42"
No. of sectors	3, 46° wide
Spiral constant	1/13 rad/inch
Minimum hill gap	2.5"
Maximum valley gap	18"
Minimum-maximum operating fields	30-50 kG
Yoke height	117"
Yoke inner and outer diameters	118"-174"
Total iron weight (poles included)	≃ 260 tons
R.F. frequency range	9-32 MHz
Harmonic operating modes	1st, 2nd
Peak dee voltage	200 kV
R.F. power per dee	< 150 kW
No. of trim coils	22
Maximum total trim coil power	≃ 60 kW

Two peculiar features of the sector geometry are apparent from Fig. 1:

a. A counterclockwise-clockwise behaviour of the spiral, with a transition radius at about 15", which is required for stripping the injected particles in a hill. A detailed discussion of this aspect of the design is given in Ref. 2.

b. A radial cut of the profile from a radius of 40.8" to 42". This, as discussed in detail below, is needed to reduce ν_z values in the extraction region, thus avoiding a dangerous intrinsic resonance.

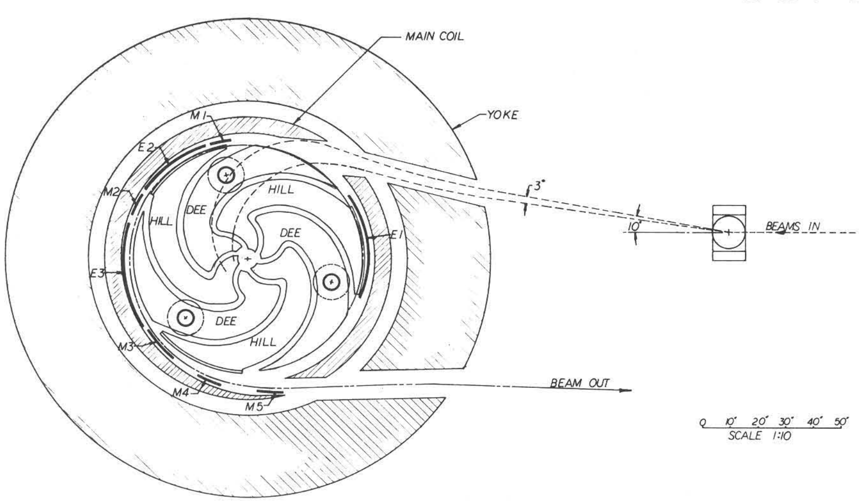

Fig. 1. Schematic layout of the K=800.

A central hole of 7" diameter is provided for insertion of the stripping foil position mechanism. Dee stems are inserted through 13" diameter holes at a radius of 31". Preliminary R.F. engineering studies indicate that, for the required 9 to 32 MHz range, the short circuit will have to move between 60" and 240" from the median plane, and therefore outside the yoke. It is anticipated that in this region the outer coaxial will be 18" diameter, and the inner one 8" diameter. The power figure quoted in Table I should be regarded at this stage as an upper limit.

*This material is based upon work supported by the National Science Foundation under Grant No. Phy 78-01684.

0018-9499/79/0400-2078$00.75

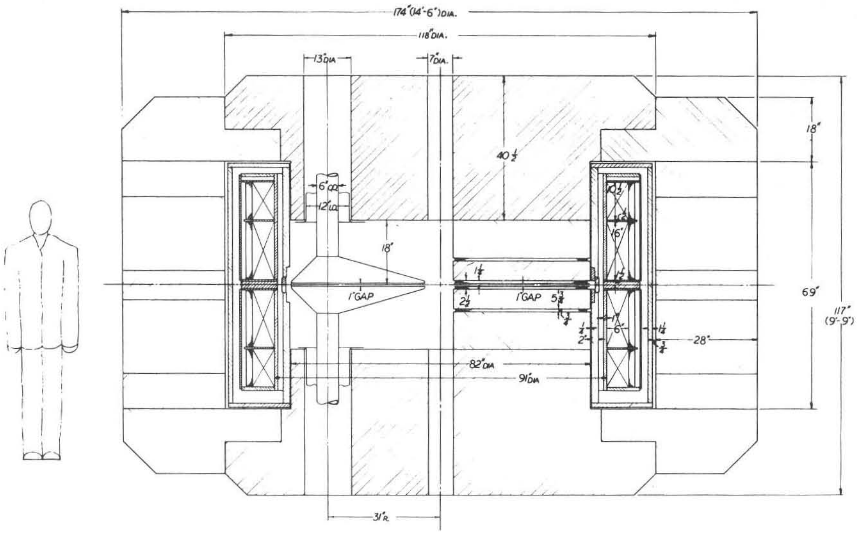

Fig. 2. Section through the magnet of the K=800.

Table II. Coil parameters

Inner coil radius = 45.5"
Outer coil radius = 51.5"
Coil total height = 26.5"
Coil splitting: two sections
Height of section closer to the median plane = 16"
Minimum coil distance from median plane = 1.5"
Maximum current density = 3500 A/cm^2
Ampereturns at maximum current = 7.2 x 10^6
Conductor: Nb-Ti, to be selected
Cryostat inner radius = 41.25"
Cryostat outer radius = 58.25"
Cryostat total height = 68"

Main coil parameters are listed in Table II, and the coil cross section is sketched in Fig. 2. Since a detailed report of the method which led to the coil design is given in Ref. 3, we shall just note here that two section splitting of the coils has been chosen. The larger section is the one closer to the median plane, with a fractional height equal to 0.6 of the total height. This design effectively reduces the total maximum trim coil power needed throughout the cyclotron operating range to about 60 kW for 22 trim coils. The latter, as schematically shown in Fig. 2, have a construction scheme similar to that of the K=500 cyclotron,[4] i.e. they are made of ¼" × ¼" square conductor wrapped around the hills in 2 layers of 5 turns each. Maximum current in each trim coil will be 300 A.

As shown in Fig. 1, extracted and injected beams run almost parallel outside the machine. This turned out to be the only practical scheme, since injection has to be through a valley with beams converging to a common point located about 150" from the cyclotron center[2]. Matching to all required injection paths can be obtained by 3° steering at this point. On the other hand, extraction requires three deflectors and five magnetic channels, over an azimuthal range of 328°, as shown in Fig. 1. Compatibility between injection and extraction leads thus to the present choice.

We turn now to a discussion of the most interesting aspects of the machine operation.

Beam Acceleration

The appearance of the ν_z=1.5 stopband, at radii around 41", was quickly recognized. Its onset is due to the simultaneous presence of a strong alternating gradient effect due to the spiral, and the fast fall-off of the fringing field. Since the stopband is impassable, extraction has to take place before then. However, acceleration runs uncovered the presence of another resonance, the $\nu_R+2\nu_z=3$ (three being the number of the sectors) which is reached well before the ν_z=1.5 stopband. This is shown in the operating (ν_R,ν_z) diagram of Fig. 4, both for 200 MeV/n and 20 MeV/n beams. Existence of such a resonance has been known for a long time,[5] although the conditions for its onset probably never materialized in a three-sector machine. This resonance being of the third order in the Hamiltonian and intrinsic, it is very nearly impassable. Effects on the axial motion can be seen in Fig. 5 for a perfectly centered beam (curve 1) and two beams where a precessional radial oscillation has been excited by a field first harmonic of amplitude 4 and 6 Gauss. Since traversal of the ν_R=1 resonance occurs well before the $\nu_R+2\nu_z=3$ resonance, it is quite obvious that the latter cannot be crossed.

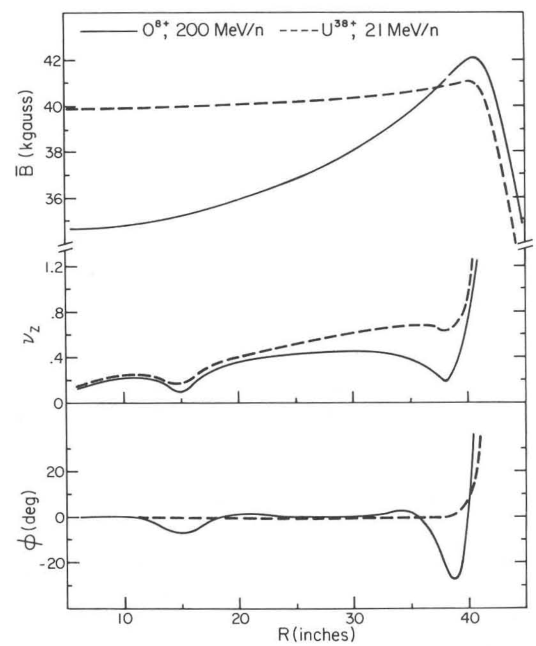

Fig. 3. Average field, ν_z and phase for 200 MeV/n and 20 MeV/n ions.

Analysis of the effective field index experienced by a particle along the equilibrium orbit, as shown in Fig. 6, curve 1, demonstrates that the simultaneous presence of the rapidly decreasing fringing field and the alternating gradient effect due to the spiral is again responsible for the high ν_R and ν_z values. On the other hand, extraction before the resonance is hardly possible in this configuration since, as seen in Fig. 4, the maximum ν_R value one can reach is about .9.

Radial cuts of the hill profile were therefore tried, to reduce the alternating gradient effect, since the fringing field fall-off can hardly be influenced. This technique proved successful, as shown by curves 2 and 3 of Fig. 6. The main effect of the radial cuts is to push the operating plot, for the same values of ν_z, towards smaller values of ν_R, which is precisely what one wants in order to make extraction easier. We finally settled upon a radial cut from 40.8" to 42", producing the (ν_R,ν_z) diagram seen in Fig. 7. The new distance from the ν_R=1 line can be compared with that of Fig. 4, and extraction is now possible at a ν_R value of about .8.

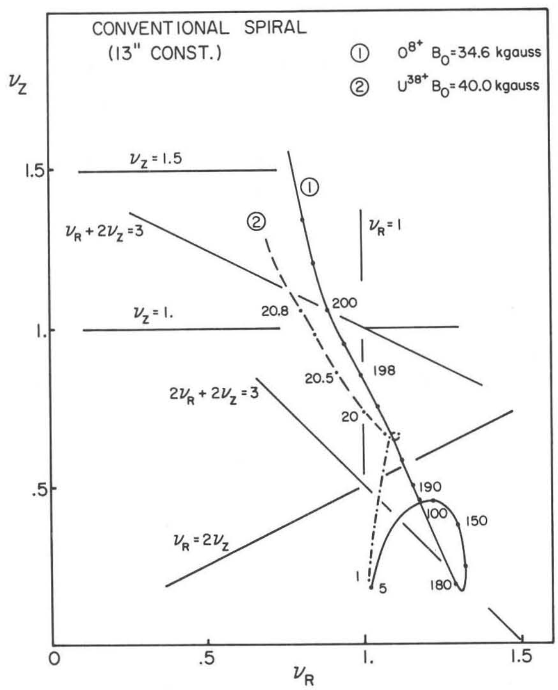

Fig. 4. Operating (ν_R,ν_z) plot for 200 MeV/n and 20 MeV/n ions with a conventional spiral.

The only other resonance present in Fig. 7, which is not usually considered in conventional AVF cyclotrons, is the $2\nu_R+2\nu_z=3$. This, however, is a fourth order resonance, and computer runs established that radial oscillations as large as 0.3" can be easily tolerated. As for the coupling resonance $\nu_R=2\nu_z$, the fact that it is traversed before the ν_R=1 resonance is indeed favourable, and radial amplitudes of .2" can be tolerated.

The appearance of the $\nu_R+2\nu_z=3$ resonance and its consequences led us to analyse very carefully the entire operating range of the cyclotron in the $(B_o,Z/A)$ space. In fact, it can be expected that at low magnetic field values the corresponding flutter increase would push ν_z to values high enough to hit the resonance at radii several inches before any reasonable extraction radius. This actually happens, as can be seen in a straightforward way in Fig. 8 for a Z/A value of accelerated particles equal to 0.5. For low enough central field values, like 25 and 27.5 kG, the resonance is in fact crossed at radii as low as 36", thus effectively prohibiting beam acceleration beyond this radius.

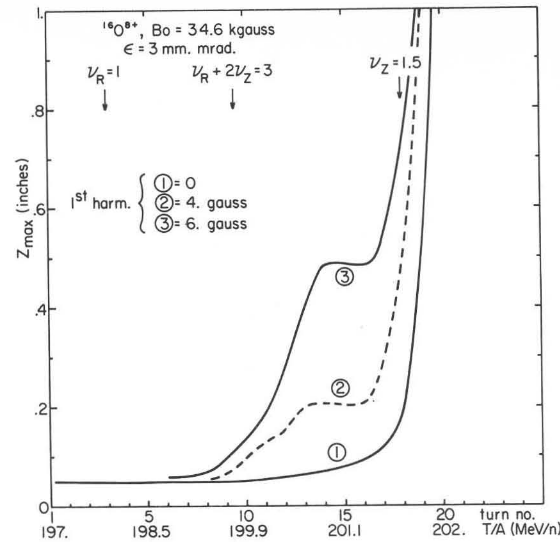

Fig. 5. Axial envelope of accelerated beam. Behavior of a centered beam (1) and of beams for which a precessional oscillation has been excited (2,3) are presented.

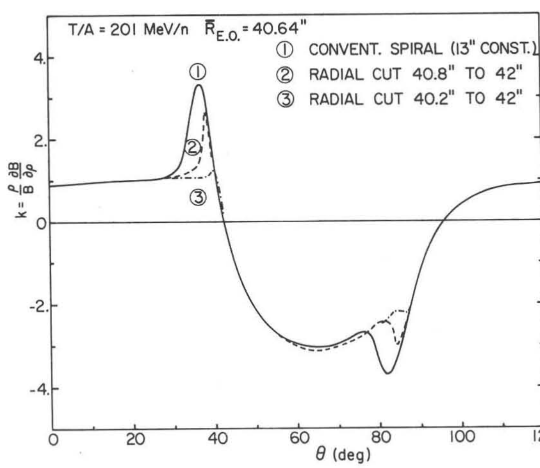

Fig. 6. Effective field index experienced by particles on equilibrium orbit (see text for details).

A number of similar calculations established that in the $(B_o,Z/A)$ plane there exists a limiting line whose equation is approximately

$$B_o\ (kG) = 35. - \frac{5}{.4}\ Z/A$$

which prevents cyclotron operation below its boundary. Consequences of this finding will be seen presently.

Coupling to the K=500 - Operating Modes

Determining the appropriate coupling modes between the two cyclotrons in order to meet design goals has proved a complex matter. Coupling of the two cyclotrons on the basis of equal R.F. acceleration frequencies obeys the following relations:

$$\frac{\beta ex_2}{\beta ex_1} = \frac{Rex_2\ h_1}{Rex_1\ h_2} \qquad (1)$$

hence

$$\frac{T_2/A}{T_1/A} \simeq \left(\frac{Rex_2\ h_1}{Rex_1\ h_2}\right)^2 \qquad (2)$$

$$\frac{Z_2\ h_2}{Z_1\ h_1} = \frac{Bo_1}{Bo_2} \qquad (3)$$

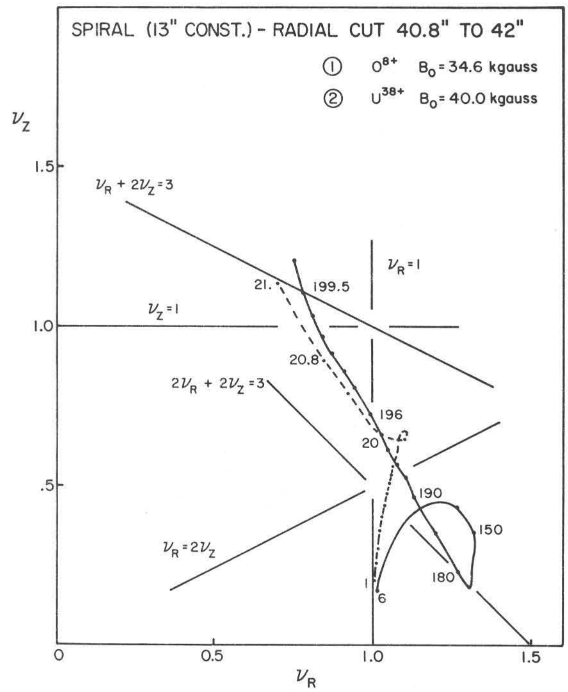

Fig. 7. Operating (ν_R,ν_z) plot with a radial cut in the spiral profile from 40.8" to 42". Same ions and fields as Fig. 4.

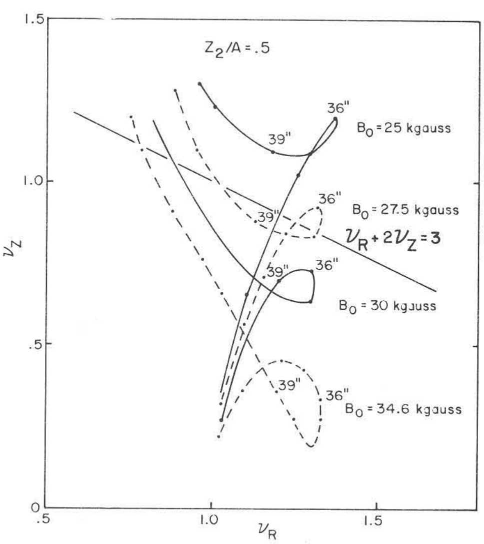

Fig. 8. Operating (ν_R,ν_z) plot for an ion with $Z_2/A = .5$ at different center field levels.

where T/A, βex, Rex, h, Z, and B_o are the extraction energy, particle velocity, extraction radius, harmonic number, charge state, and center field value of the first cyclotron (K=500) or the second cyclotron (K=800) according to the subscript. The harmonic coupling ratio $h_1:h_2$ (HCR) is therefore of paramount importance in determining the actual operating parameters.

The particle energies allowed for both machines, according to (1), are presented in Fig. 9 for all harmonic modes. It is seen that because of R.F. limits only HCR of 3:1, 4:1, or 5:1 can be considered for the high energy range, 4:2, 5:2, and 7:2 being available for the low energies. Overlap can occur in the 18 MeV/n to 60 MeV/n range.

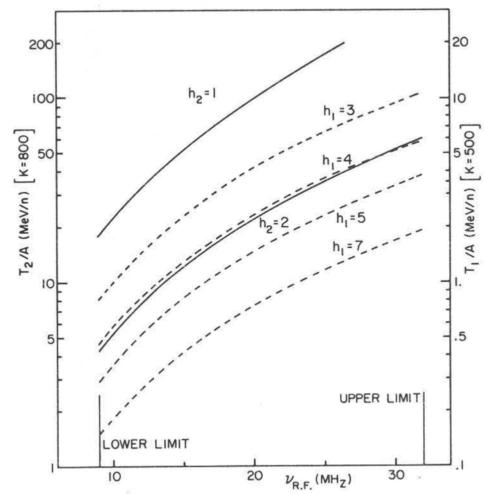

Fig. 9. Energy in MeV/n for both cyclotrons as a function of R.F. frequency for different harmonic modes.

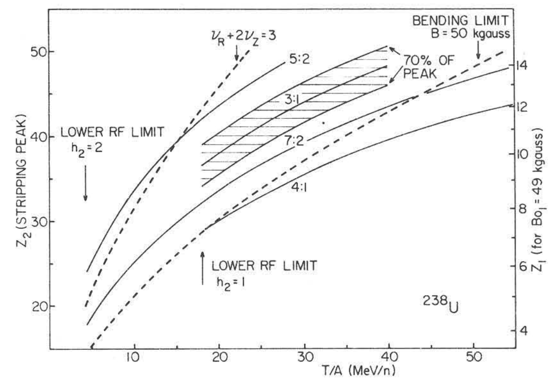

Fig. 10. Most probable charge state after stripping, for uranium, as a function of final energy. See text for details.

The appropriate coupling mode must then be studied for every single ion, keeping in mind the following requirements:

a. for the first cyclotron, the lowest possible harmonic number, h_1, and charge state, Z_1, should always be preferred for obvious beam intensity reasons.

b. The charge state or stripping ratio, Z_2/Z_1, should not only obey (3), but also correspond to the peak, or be very close to the peak, of the stripping distribution for any given injection energy.

c. Bending, focussing, and resonance limits have to be strictly observed.

How this study is actually done can be seen in Fig. 10 for the case of uranium. The most probable charge state Z_2, after stripping, is plotted as a function of the final energy for all possible harmonic coupling ratios. For the case of HCR 3:1 the band corresponding to 70% of the peak intensity is also shown, to give an idea of the limits posed by requirement (b). The scale on the right refers to the minimum charge state Z_1 allowed in the first cyclotron, according to a field center value of 49 kG, and can be used for every HCR curve. Also indicated are the $\nu_R+2\nu_z=3$ limit and the bending limit for 50 kG at extraction radius. One sees immediately that the 3:1 mode is the lowest possible over the 18 to 40 MeV/n range, the upper limit coming from charge state $Z_1=14^+$ in the first machine.

Even higher energies are possible, up to 50 MeV/n, using the 7:2 mode. One must allow departure from the maximum stripping intensity, because of the bending limit in the second cyclotron, but still stay within 70% of the peak value. At energies lower than 18 MeV/n, where the second harmonic must be used for the K = 800, the 7:2 mode is always possible, while the 5:2 mode can only be used by shifting off the peak intensity, because of the resonance.

These curves can be transformed into $(B_o, Z_2/A)$ diagrams, as shown in Fig. 11, where for each energy in MeV/n the limits within 70% of the peak intensity are drawn for every HCR. In this diagram one can appreciate not only the necessary range of magnetic fields, but also how and in which range the energy can be varied continuously by keeping a constant Z_2/A value and just varying the magnetic field.

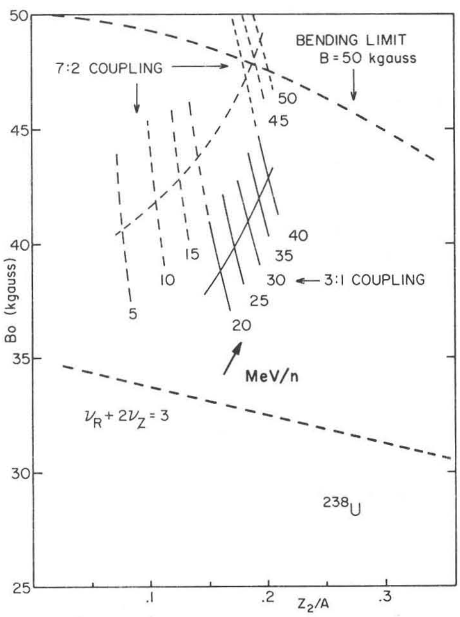

Fig. 11. Operating $(B_o, Z_2/A)$ plot for uranium. For every HCR the center line refers to the peak charge state, and crosses constant T/A lines.

Similar analyses have been made for a number of ions throughout the periodic table. When all these results are put together, one obtains the overall operating diagram in the $(B_o, Z_2/A)$ plane shown as a gray area in Fig. 12. The boundaries of the operating region are given in a self-explanatory way on the figure itself. Also shown are the operating lines for a number of representative ions, and HCR=3:1 and 7:2, corresponding to the most probable charge state after stripping.

The same analysis also determines, for each ion and HCR, the limits of the stripping ratio, Z_2/Z_1. They are presented for HCR=3:1 and for ^{63}Cu, ^{122}I, and ^{238}U in Fig. 13 as a function of the final energy per nucleon. The dashed lines correspond to constant charge state Z_1 and, for each energy, to the most probable charge state Z_2. The upper limit on Z_2/Z_1 is then given by the bending limit of the first cyclotron. The lower line is instead a possible limit for the continuous transition from one charge state Z_1 to the next one, while keeping Z_2 at the value for peak stripping intensity. It is seen from Fig. 13 that:

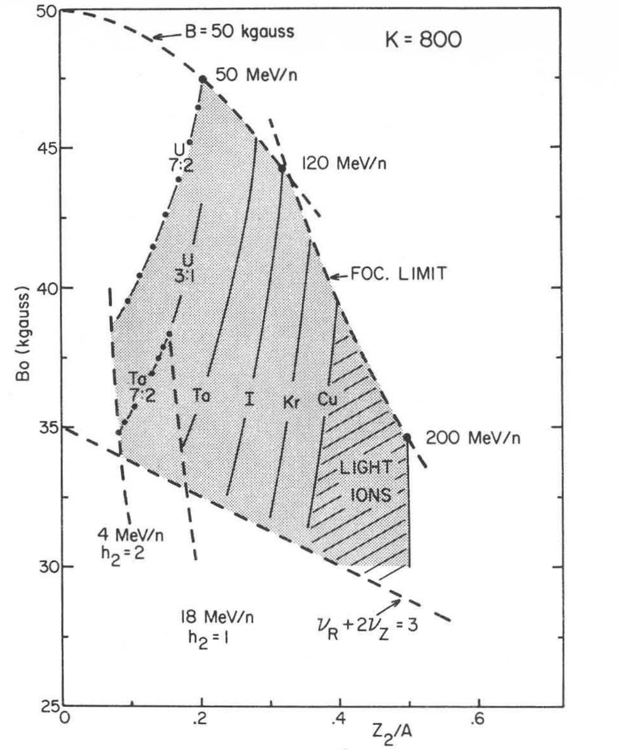

Fig. 12. Overall $(B_o, Z_2/A)$ operating diagram for the K=800.

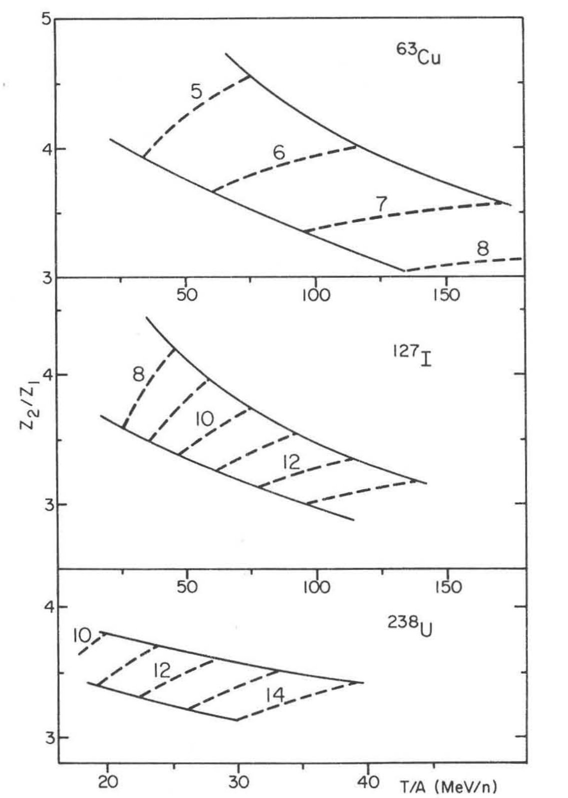

Fig. 13. Stripping ratios as a function of energy for HCR=3:1 and different ions. See text for details.

- practically the same range of Z_2/Z_1 applies for every ion.
- Z_2/Z_1 must decrease as a function of energy.
- henceforth the injection must accomodate a fairly large range of stripping ratios [2] for proper coupling of the two cyclotrons.

0018-9499/79/0400-2082$00.75 ©1979 IEEE

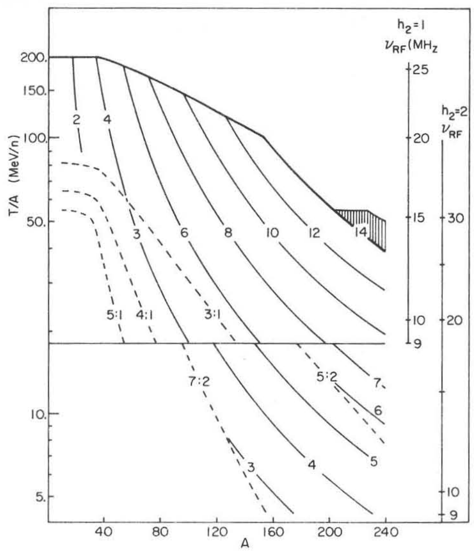

Fig. 14. T/A in MeV/n vs. ion mass number.

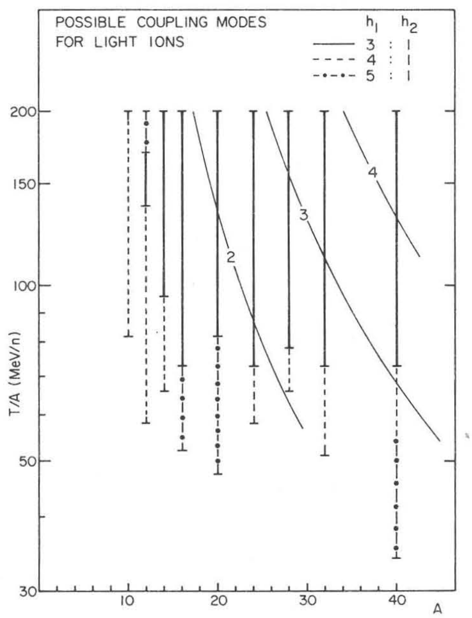

Fig. 15. T/A in MeV/n for light ions.

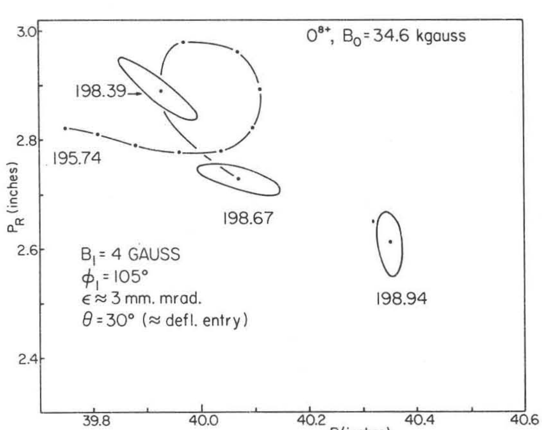

Fig. 16. Turn to turn separation at deflector entrance via excitation of $\nu_R=1$ resonance.

In the customary T/A vs. A plane, the machine performance is illustrated in Fig. 14. The limits for the various HCR, as defined by the $\nu_R+2\nu_z=3$ resonance, are shown as dashed lines. At 18 MeV/n, i.e. 9 MHz, there is the lower limit for first harmonic operation. The bending limits of the K=500 are also shown for a number of charge states Z_1 and, for $Z_1=14^+$, they determine the machine characteristic for $A\geq150$. The dashed region for $A\geq200$ corresponds to the possible use of the 7:2 HCR as discussed above for uranium. The focussing limit, $K_F=400$, defines the maximum energies for A<150. An enlarged scale diagram is given for light ions in Fig. 15, details being noted on the figure in a self explanatory way.

From this analysis the following main conclusions can be drawn:

- The 3:1 HCR can and should be used over most of the high energy range. The presence of the $\nu_R+2\nu_z=3$ resonance does, however, severely restrict its use at low energies for light and medium ions, where a switch to 4:1 or 5:1 mode is compulsory. Likewise, the 2:1 mode is really not interesting since its limits are obviously higher than for the 3:1 mode.
- For energies below 18 MeV/n, the 5:2 mode has a very narrow range in terms of T/A vs. A, and the 4:2 mode is therefore not practical. The 7:2 mode can instead be used over a very wide range. Should energies below 18 MeV/n be desired for mass numbers below 100, one should resort to even higher harmonic modes in the first cyclotron. Their practical feasibility has not, however, been investigated yet.

As for the operating region of the first cyclotron in the $(B_{ol}, Z_1/A)$ plane, we have found that Z_1/A should range from 0.02 to 0.15, with magnetic field values spanning from 30 to 49 kG.

Beam Extraction

Extraction studies have been concentrated so far on a careful analysis of the 200 MeV/n case. The extraction scheme, as shown in Fig. 1, consists of three deflectors positioned in two consecutive hills and a valley, and five magnetic channels. The latter are of the passive type, i.e. saturated iron bars, and therefore produce both a negative bias field and a radially focussing gradient. Parameters for all elements as used in the extraction of 200 MeV/n beams are given in Table III.

Table III. Extraction scheme characteristics.

Element	$\Delta\theta$ (deg.)	E. field (kV/cm)	$-\Delta B$ (kG)	$\partial B/\partial x$ (kG/inch)
E_1	58^o	140.	---	---
M_1	10^o	---	2.	5.8
E_2	36^o	140.	---	---
M_2	12^o	---	2.	5.8
E_3	50^o	140.	---	---
M_3	18^o	---	2.	5.8
M_4	10^o	---	2.	5.8
M_5	10^o	---	2.	9.0

Excitation of the $\nu_R=1$ resonance via a field first harmonic is used to produce sufficient turn separation at the deflector entry, as shown in Fig. 16. Proximity of the $\nu_R+2\nu_Z=3$ resonance demands however considerable attention in choosing a not too far out extraction radius, because deterioration of the axial phase space sets in quickly. For example, for the particular field level to which Fig. 16 refers, the energy of 199 MeV/n corresponds to ν_R and ν_Z values of .81 and 1.03 respectively, thus comfortably away from the resonance. The resulting axial phase space at the deflector entry is then shown by the solid line in Fig. 17. If, at the same field level, extraction is attempted at an energy of 199.5 MeV/n, which corresponds to a deflector entrance radius of 40.55" (i.e. .2" farther out), then the axial phase space turns to the dashed line of Fig. 17. At this radius, in fact, ν_R and ν_Z are .78 and 1.1 respectively, thus very close to the resonance.

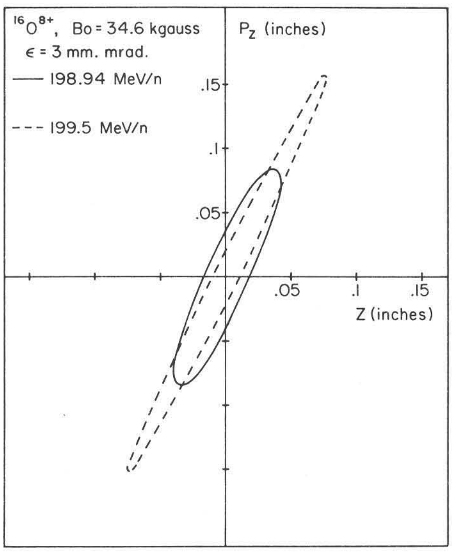

Fig. 17. Axial phase space at deflector entrance for two different particle energies. See text for details.

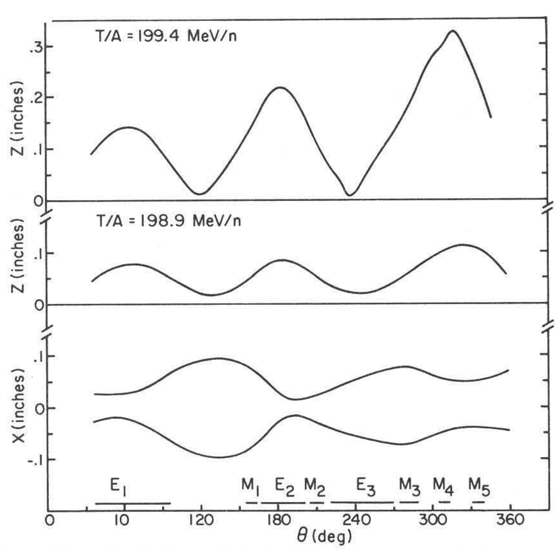

Fig. 18. Radial and axial envelopes of the extracted beam. See text for details.

Extracted beam envelopes are shown for both these cases in Fig. 18. It is seen that the beam extracted at 40.35" is extremely well confined, both radially and vertically, to within ≃.1", while the beam extracted at 40.55" would be more spread out vertically. Obviously the former solution has been chosen, since gains in somewhat lower electric fields, or faster extraction, do not really make up for the worse beam behaviour.

The present extraction scheme has been tested for other cases of particles and energies, showing that extraction is indeed always possible with, of course, reduced electric fields for less relativistic particles. Typically, electric fields of 130 kV/cm are needed for the extraction of iodine at 110 MeV/n, and 30-40 kV/cm for uranium at 20 MeV/n. At this stage it is believed that the deflectors will have to be radially movable, approximately within ≃.1", in order to allow extraction with a practically constant exit trajectory over the whole operating range. This point will need, however, a much more detailed investigation. Field perturbation produced by the magnetic channels will be compensated in a way similar to that used for the K=500 cyclotron.

Summary

A list of typical beams and operating parameters is given in Table IV as an assessment of overall machine performance.

Table IV Typical beams.

Ion	T_2/A (MeV/n)	T_1/A (MeV/n)	h_1/h_2	ν_{RF} (MHz)	Z_2/Z_1	% strip.	Bo_2 (kG)	Bo_1 (kG)
^{16}O	200	7.2	3/1	26.6	8/2	70	34.6	46.1
^{16}O	100	4.1	3/1	20.1	7/2	30	29.9	34.9
^{63}Cu	160	6.1	3/1	24.4	25/7	27.	40.0	47.6
^{63}Cu	80	3.4	3/1	18.2	23/6	27.	32.5	41.6
^{127}I	110	4.5	3/1	20.9	40/12	20.	43.3	48.1
^{127}I	70	3.0	3/1	17.2	37/10	20.	38.4	47.4
^{238}U	50	1.6	7/2	29.5	49/14	11.	46.6	46.6
^{238}U	40	1.3	7/2	26.6	44/12	15.	46.8	49.0
^{238}U	30	1.4	3/1	11.6	44/13	15.	40.8	46.1
^{238}U	20	.9	3/1	9.5	38/10	15.	38.9	49.3

In summary, this study shows that the design of a superconducting cyclotron for a range of energies and particles like the one aimed at in this project has to be pursued in great detail, just to establish an effective feasibility. In particular, an energy of 200 MeV/n for fully stripped ions looks close to the upper practical limit for a three sector machine. On the other hand, problems like extraction, isochronous field trimming, and injection can be solved without undue construction difficulties, or in other words, in a way similar to that in use for lower energy superconducting cyclotrons.

As an overall conclusion, the present results look firm enough to justify the detailed engineering study which would be needed to produce a final design of the K=800 cyclotron.

References

[1] H.G. Blosser et al., MSUCL-222A, Sept. 1976, unpublished.

[2] G. Bellomo, E. Fabrici, and F. Resmini, "Injection studies for the K=800 superconducting cyclotron at MSU," paper at this Conference.

[3] G. Bellomo and F. Resmini, "A method for minimizing trim coil power requirements in a superconducting cyclotron," paper at this Conference.

[4] H.G. Blosser, D. Johnson, and R.J. Burleigh, "Proceedings of VII Int. Conf. on Cyclotrons (Birkhauser, Basel, 1975) p. 584.

[5] M.M. Gordon, Annals of Physics 50, 571 (1968).

0018-9499/79/0400-2084$00.75 ©1979 IEEE

** DISCUSSION **

J. RICHARDSON: The rule $[\omega RF]_{1st\ stage} = [\omega RF]_{2nd\ stage}$ is not a real requirement. In our kaon factory design, we go from 23 MHz in TRIUMF to twice the frequency with flat topping. This is quite satisfactory.

F. RESMINI: The requirement of equal R.F. frequencies is the most simple and straightforward way to match the two cyclotrons. You are quite correct in pointing out other possibilities.

J. BALL: Your plot of the operating limit region showed an upper limit bounded by a 50 KG bending limit. This would correspond to an energy constant larger than K=800.

F. RESMINI: You are quite right. For uranium ions, if the 7:2 harmonic coupling is used, 50 MeV per nucleon can be reached, corresponding to a K≃1200. But let me point out that we have not tried to design a K=1200 machine. It is simply that the optimized coils which are needed to produce isochronism between 200 MeV per nucleon and 4 MeV per nucleon give you enough margin to be able to produce for these middle-of-the-road relativistic particles 50 MeV per nucleon.

T. KUO: In three superconducting cyclotron papers this morning I observed that there are holes in 3-fold symmetry bored through each valley to accommodate the dee systems. Would you comment on the effect of these holes on the magnetic field in the valleys?

F. RESMINI: The average magnetic field is obviously slightly reduced by a few hundred gauss and some effect is apparent, of course, also in the field modulation. However, cyclotron performance is essentially unaffected.

W. DAVIES: Your injection orbits cross the poles in a complicated fashion. This could produce wildly varying optical properties for injection. Could you comment on this problem?

F. RESMINI: I did not have the time to cover phase space behavior of injected beams. This looks, however, very reasonable, and is covered in another paper at this conference. There is no sign of distortion in the phase space, and there is no excessive defocusing in the cyclotron fringing field.

0018-9499/79/0400-2085$00.75 ©1979 IEEE